Electrostatic Effect on Electron Transfer at the Active Site of Heme Peroxidases: A Comparative Molecular Orbital Study on Cytochrome C Peroxidase and Ascorbate Peroxidase

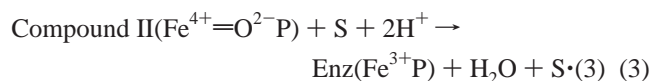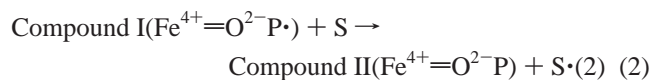### Dóra K. Menyhárd and Gábor Náray-Szabó*

Department of Theoretical Chemistry, Eötvös Loránd University, H-1117 Budapest, Pázmány Péter st. 2, Hungary

Received: April 7, 1998

Ab initio minimal basis set molecular orbital and discretized Poisson−Boltzmann electrostatic potential calculations were carried out on large models of the active site of heme peroxidases (cytochrome C peroxidase and cytosolic ascorbate peroxidase) to rationalize the location of the radical site in Compound I, an intermediate of the enzymatic reaction. Both molecular orbital and electrostatic potential calculations suggest that the spin distribution depends on the protonation state of the proximal His...Asp...Trp triad. If the transferable proton is shifted from the Trp side chain to Asp, the radical localizes on the indole group, while if it remains on the Trp the unpaired electron transfers to the heme group. Therefore, in cytochrome C peroxidase, Trp is deprotonated in Compound I, while it is protonated and neutral in cytosolic ascorbate peroxidase. Protonation state of the proximal residues is influenced by the electrostatic effect of the protein environment that differs in these enzymes, especially in the immediate vicinity of the Asp side chain. In contrast to earlier propositions we did not find evidence for the effect of the neighboring potassium-binding loop on the localization of the free radical. The heme peroxidases studied provide examples for the electrostatic, protonation-mediated modulation of electron transfer.

Introduction

Peroxidases are heme-containing metalloenzymes which catalyze a great variety of oxidation reactions. They share a common ability to react with H_2O_2 and form relatively stable active states, storing oxidizing equivalents in their ferryl-oxy unit and in the protein itself. The reaction with H_2O_2 is a two-electron oxidation process that would result in an Fe(V)=O moiety, but by electron transfer from the protein Compound I with an Fe(IV)=O center and an organic radical is formed, that is transformed back to the ferric state via Compound II:

$$Enz(Fe^{3+}P) + H_2O_2 \rightarrow Compound\ I(Fe^{4+}=O^{2-}P\cdot) + H_2O \quad (1)$$

$$Compound\ I(Fe^{4+}=O^{2-}P\cdot) + S \rightarrow$$
$$Compound\ II(Fe^{4+}=O^{2-}P) + S\cdot(2) \quad (2)$$

$$Compound\ II(Fe^{4+}=O^{2-}P) + S + 2H^+ \rightarrow$$
$$Enz(Fe^{3+}P) + H_2O + S\cdot(3) \quad (3)$$

In most peroxidases, like pea cytosolic ascorbate peroxidase (Apx), the radical is located at the porphyrin ring, while in cytochrome *c* peroxidase (CcP) it localizes at a nearby Trp side chain (191 or 179 in Figure 1). Location of the radical is of functional importance, since peroxidases reduced at the porphyrin ring react with a variety of small organic[1,2] and inorganic[3,4] molecules and ions, while CcP radicalized at Trp-191[5,6] reacts with bulky cytochrome *c*[7] which is not able to reach the buried porphyrin site but easily reacts with a more surface close radical.

The distal heme pocket of peroxidases forming the peroxide-binding site contains a conserved His and an Arg residue which are required for activity.[8] The proximal pocket contains the invariant His heme ligand which forms a hydrogen bond with a conserved Asp side chain. Directly adjacent to these is a nonpolar group which is Phe in most peroxidases, but CcP and Apx have a Trp at this location, also H-bonded to Asp.

Despite their very similar active site structure and 33% global sequence identity[9] CcP is radicalized at the Trp of the proximal side, while Apx forms a porphyrin radical.[10] Based on the comparison of the two crystal structures, Poulos and co-workers[11] proposed that a K^+ ion of Apx captured in place of a water molecule of CcP is responsible for the shift of the radical center. To test this hypothesis they engineered a similar cation-binding site in CcP[11] but the effect was only a destabilization of the Trp radical while no radical at the porphyrin ring could be detected. Therefore it still remains a question why these two enzymes, containing very similar active-site structures, behave so differently when activated.

The neutral or positive character of the Trp radical of CcP has also been investigated by various methods which did not provide an unanimous answer. Kraut and co-workers demonstrated in a mutation study[12] that replacement of Trp-191 of CcP by Gly leaves a large hole in the crystal structure that is partially occupied by a cation, therefore they concluded that a cationic Trp radical is favored. ENDOR results of Huyett et al.[13] pointed in the same direction. However, Krauss and Garner, based on the UV spectrum of the radical, argued in favor of a neutral Trp side chain.[14]

Recently we hypothesized on the basis of semiempirical molecular orbital calculations[15] that both the close surrounding and the protein bulk electrostatically stabilize different proton-
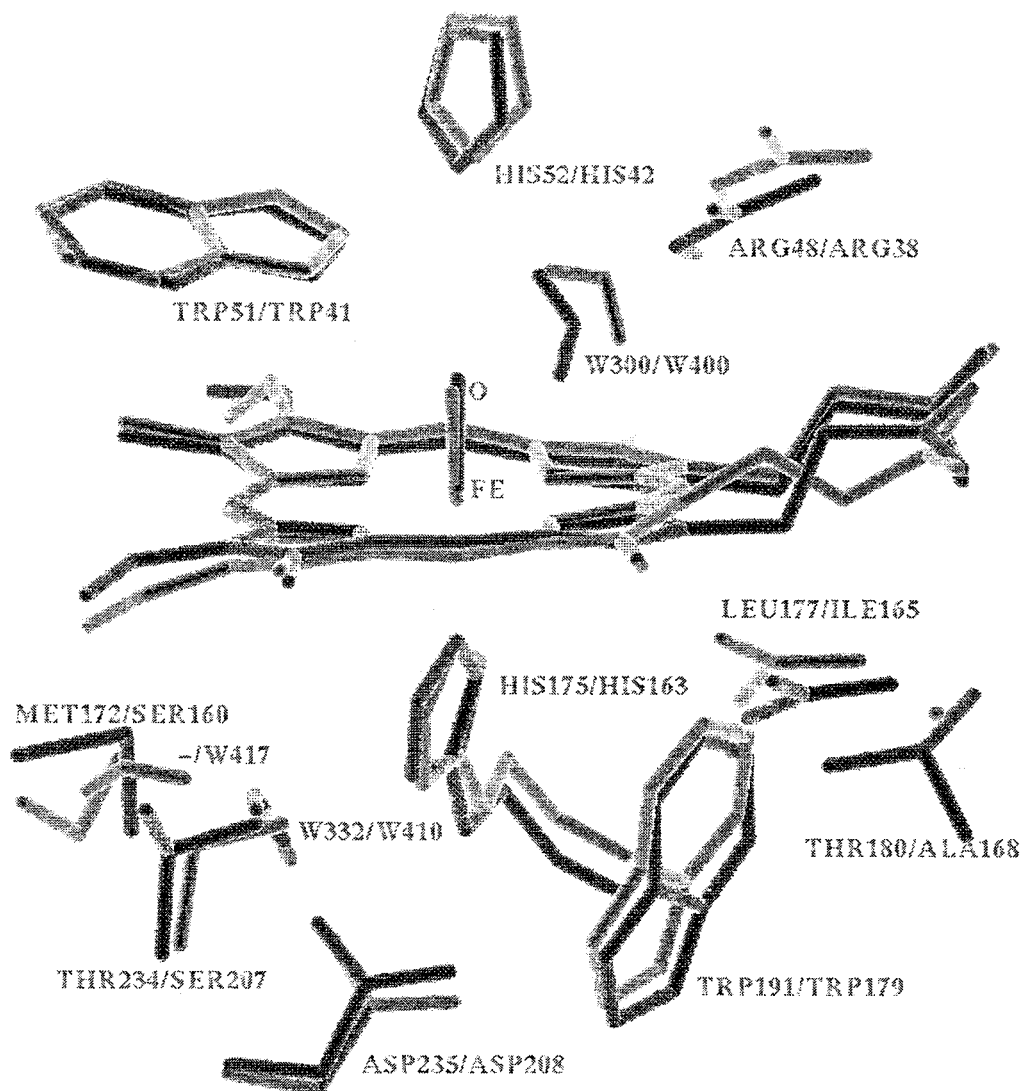
Figure 1. Computer model of the superimposed active sites of CcP (black) and Apx (grey).

ation states of the three H-bonded amino acids of the proximal side in CcP and Apx, thus modulate the location of the free-radical center. In this work we report on a higher-level study of this hypothesis based on ab initio minimal basis set molecular orbital and discretized Poisson–Boltzmann calculations on large models of the two enzymes.

Models and Methods

Geometric models of CcP and Apx were taken from the Protein Data Bank.[16] Since the active site groups of CcP and Apx are identical (ferryl-oxy heme, distal side amino acids: Arg, Trp, and His, proximal His residue, H-bonded Asp and Trp side chains), a quite large model of both enzymes (205 atoms for CcP, 198 atoms for Apx) had to be considered in order to include those structural units that might account for the different behavior of the two enzymes (see Figure 1). The following residues of CcP, lying close to the active site, are different in Apx: Met-172→Ser-160, Thr-234→Ser-207, Leu-177→Ile-165, Thr-180→Ala-168. Because of the Met/Ser (apolar/polar) switch, an additional water molecule (W-417) binds at the active site of Apx, which is H-bonded to both Ser-160 and the water molecule replacing the one present in CcP. These changes result in a quite different electrostatic milieu around the His-175/His-163...Asp-235/Asp-208 pair. Amino acids were included without

backbone atoms except for His-175/His-163 (CcP/Apx) where the carbonyl group was also built in the model. This was necessary since it has been shown that spin delocalization might occur from Trp to this nearby carbonyl,[17] that is suspected to be one of the groups providing electrostatic stabilization of the Trp radical.[12] For this reason[17] we also included Leu-177 and Ile-165 in our models for CcP and Apx, respectively. Both propionates of the heme group were protonated in all models.[18]

Because the crystal structure of Compound I for Apx has not been determined yet, models were derived from the respective resting state structures[11,19,20] by the same procedure in both cases. Iron was moved into the heme plane and the oxygen was placed 170 pm from it in a perpendicular orientation, in accordance with crystallographic results[21,22] for Compound I of CcP. We treated three types of models. In the first model, calculations were done for the bare active site with around 200 atoms (cut out from the enzyme with dangling bonds saturated by hydrogen atoms); in the second one we also included point charges of those enzyme atoms in the Hamiltonian of the quantum mechanical calculation that lie in the vicinity of the active site, while in the third one we treated full models including active site, heme, protein environment, and surrounding biophase; however, we considered only classical electrostatic effects via solution of the Poisson–Boltzmann equation.
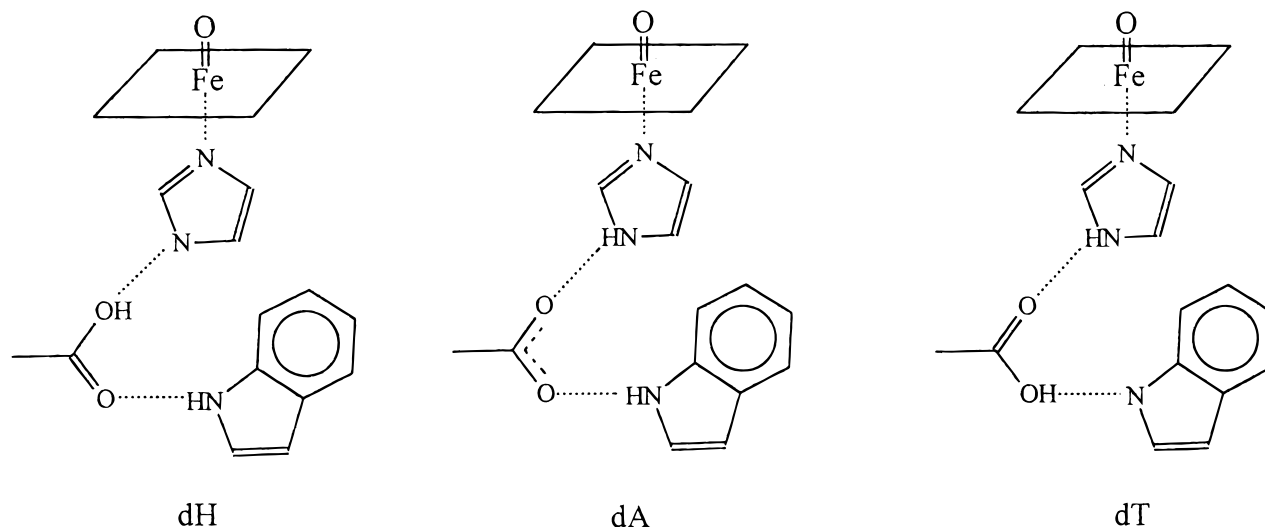
Cytochrome C Peroxidase and Ascorbate Peroxidase

J. Phys. Chem. B, Vol. 103, No. 1, 1999 **229**

Figure 2. Possible protonation states of the proximal His...Asp...Trp triad in CcP and Apx. dH: His deprotonated, dA: Asp deprotonated, dT: Trp deprotonated.

Owing to their extremely large size only the simplest ab initio methods could be applied for the first two models. We did calculations using our high-performance IBM Scalable Parallel 2 computer system with 256 MB RAM, but even this allowed only unrestricted Hartree−Fock (UHF) calculations with a minimal basis set that were carried out using the Gaussian94 progam.[23] The approach is not appropriate for the determination of probable protonation sites; however, it reproduces qualitatively the shift of the spin-density distribution coupled to proton transfer in organic radicals,[24] thus it seems to be adequate to tackle the present problem of radical location. Experiments indicate that Compound I of CcP is a quartet;[6] therefore, calculations on both CcP and Apx were carried out for this spin state. We carried out single-point calculations at fixed geometries, derived from the data set of the Protein Data Bank.[16] The two mobile protons of the His-175/His-163...Asp-235/Asp-208...Trp-191/Trp-179 triad were placed at their three possible positions at standard geometries. The above models correspond to deprotonated His (dH), deprotonated Asp (dA), and deprotonated Trp (dT) states, respectively.

The effect of surrounding protein residues was considered by treating their atoms as point charges in a second set of minimal basis set molecular orbital calculations. Kollman charges[25] were assigned to the selected residues and they were included in the calculation via the Massage command of Gaussian94 allowing incorporation of them in the Hamiltonian. The cation-binding loop of Apx was modeled by Thr-164, Thr-180, Asn-182, Ile-185, Asp-187, and a K^+ cation. The similarly positioned loop of CcP occupied by a water molecule was constructed by Ala-176, Gly-192, Ala-194, Val-197, and Thr-199. The mutation study carried out by Poulos and co-workers[11] was modeled by the following virtual mutations in CcP: Ala176Thr, Gly192Thr, Ala194Asp, Thr199Asn, and by including a K^+ ion in place of the originally coordinated water molecule.

Electrostatic calculations for the entire protein were carried out by solving the discretized Poisson−Boltzmann equation[26,27] using the DelPhi program package.[28] Both enzyme models were divided into four regions as follows: (a) atoms of the H-bonded His... Asp...Trp triad as shown in Figure 2 and represented by Kollman charges (modified for deprotonated Trp where no such charges are available, thus the proton charge of 0.2 electron units was added to that of the deprotonated nitrogen, NE1); (b) the heme unit including the iron and active oxygen atoms

represented by Mulliken charges (no Kollman charges are available) which were obtained from our ab initio minimal basis set calculations; (c) the rest of the protein, again modeled by Kollman point charges[25]; and (d) the biophase containing water and counterions, the latter following a Boltzmann distribution. The total free energy of solvation of the triad by the rest of the protein was calculated as the sum of desolvation (interaction with a dielectric representing the protein) and interaction free energy terms (with protein charges). Desolvation energy equals half of the energy difference created by the transfer of the triad from water to the uncharged protein. The interaction term was calculated from the potential created by the triad at the uncharged protein atomic sites. Calculations were focused in four steps to a final state where 90% of the calculation box was filled by the protein, the internal (protein) and external (water) dielectric constants were set to 4 and 80, respectively, and the ionic strength was chosen to be 0.1. These are the proposed standard values.[26,27] The electrostatic potential generated at the atomic sites of the triad was calculated by placing the three uncharged residues into the charged protein.

Results

Protonation States. Results of ab initio calculations are summarized in Table 1. It can be seen that in most cases (with the exception of the dH state of Apx) the total spin of $S = 3/2$ (total spin density of 3) is distributed among three species: the ferryl-oxy unit, the porphyrin ring, and the proximal tryptophan residue. If we go along the course of the transferable proton starting from a deprotonated His (dH) in the case of CcP we see that initially the porphyrin ring system is radicalized along with the ferryl-oxy center, when deprotonating Asp (dA state) we see all the spin localized on the iron and the active oxygen. At last, deprotonation of Trp (dT state) results in a spin-density distribution split in an approximately 2:1 ratio between the ferryl-oxy unit and the proximal Trp, this is the experimentally detected state. In the case of Apx, upon deprotonation of His (dH) the calculated spin-density distribution was centered on the ferryl-oxy unit, the porphyrin, and the distal Trp side chain. Although detailed analysis of the energies of different protonation states is not very meaningful in the case of minimal basis set UHF calculations, the large excess energy of this arrangement as compared to the other two makes its occurrence highly unlikely. This is further supported by the fact that in case of

TABLE 1: Calculated Spin Densities (*qs*, electron units) and Total Energies (*E*, a.u.) As Obtained for the Three Different Protonation States of the Proximal His...Asp...Trp Triad in CcP and Apx

	CcP			Apx		
	dH	dA	dT	dH	dA	dT
qs(Fe=O)	1.97	3.10	2.05	1.04	1.73	1.99
qs(porphyrin)	1.27	−0.07	−0.11	1.02	1.30	0.04
qs(Trp)	0.02	0.00	1.05	0.01	0.00	1.03
qs(His carbonyl)	−0.03	0.00	0.08	0.00	−0.01	0.00
E	−6181.193	−6181.041	−6181.247	−5743.564	−5747.188	−5747.216

TABLE 2: Comparison of Calculated and Experimental Spin-Density Distributions for the Neutral and Cationic Form of the Trp Side Chain in CcP

	neutral Trp radical (dT state)				cationic Trp radical	
		ref 13			ref 13	ref 14
atom	calcd	calcd	ENDOR	ref 14	ref 13	ref 14
N1	0.75	0.30	0.12	0.77	0.04	0.08
C2	−0.69	0.04	0.35	0.00	0.42	0.24
C3	0.87	0.39	0.41	0.13	0.39	0.40
C4	−0.32			0.01		0.09
C5	0.35	0.09		0.02	0.10	0.00
C6	−0.20	0.03	0.07	0.00	-0.04	0.08
C7	0.27	0.06		0.04	0.09	0.04
C8	−0.07	0.08		0.00	-0.01	0.04
C9	0.08			0.03		0.01

the dH protonation motif a considerable part of the total spin density is located on the distal Trp-41 of Apx, which was never experimentally detected as a radical site. Deprotonation of Asp (dA state) results in radical formation both on the porphyrin ring and the ferryl-oxy group (this is the experimentally detected state), while, as in CcP, the dT state is a proximal Trp and ferryl-oxy radical. If we compare these results to the experimentally determined spin distributions of Compound I of CcP and Apx, we obtain evidence that in CcP the Trp should be deprotonated by the H-bonded Asp residue, while in Apx the opposite happens, Trp holds on to its proton and Asp is ionized.

Spin Distributions of CcP dT and Apx dA States. Details of the calculated spin density of the experimentally detected tryptophan radical of CcP (dT state) and that of the porphyrin radical of Apx (dA state) are presented in Tables 2 and 3. For the tryptophan radical of CcP, results of previous calculations[13,14] for isolated neutral and cationic indole radicals along with experimental results[13] are also displayed. In CcP all heteroatoms of the Trp radical carry a considerable spin density, while in Apx the spin on the nitrogen atoms and the carbon atoms connecting the pyrrole rings makes up for most of the spin density of 1.3 of the porphyrin ring.

Charges. Although most negatively charged groups suspected of stabilizing a cationic Trp radical were included in our model, we did not find a net positive charge on this residue for any of our models. In contrast, we found that the Trp of the proximal side is radicalized only if it is deprotonated, i.e., neutral. If Trp is deprotonated and radicalized (dT state) in CcP, it carries practically no charge both in CcP and Apx. If the proton is on Trp then the unpaired spin localizes at the porphyrin ring, or in the case of CcP at the ferryl-oxy center alone; therefore, the charge of the Trp residue remains close to zero (−0.04 electrons) in both enzymes, while Asp carries a formal negative charge (−0.87 and −0.89 in CcP and in Apx, respectively).

Spin Delocalization to the Main Chain Carbonyl Group of the Proximal His. Spin delocalization to the main chain carbonyl group of the proximal His was observed only for the deprotonated state of Trp in CcP. The spin density on the carbonyl atoms in absolute value is considerable (0.702 and −0.620 on C and O, respectively) but opposite in sign, which

results in a quite modest, but still the largest amount of spin density calculated for this group.

Effect of the Water/Cation Binding Loop on the Spin-Density Distribution. One of the remarkable differences between the crystal structure of CcP and Apx is that a cation-binding loop can be found in the latter, occupied by a potassium cation, while this position is occupied by a water molecule in CcP. The potassium ion is located at 1.35 nm from the Fe atom, approximately 1.3 nm from both Asp oxygen atoms and 1.07 nm away from NE1 of Trp. We studied the electrostatic effect of this loop on the spin density of the proposed Compound I structure, dT, of CcP (see Table 4). Adding the water-containing loop to the model as point charges, and recalculating the dT state of CcP did not alter the spin-density distribution. Replacing these amino acids with a K^+-binding loop similar to that in Apx, the dT protonation scheme still resulted in a Trp radical of overall spin density of approximately 1; however, the absolute spin density values on the benzene ring of Trp did change, they all increased by more than a factor of 3. This result is in accordance with the experimental finding of Poulos and co-workers[11] that an engineered cation-binding site did not radicalize the porphyrin ring in Compound I, only lead to the rearrangement and destabilization of the Trp radical center. The above results seem to demonstrate that the potassium binding loop does not directly affect the spin distribution in Compound I.

Electrostatic Potential Calculations by DelPhi. CcP and Apx are similarly folded, but from the point of electrostatics quite different proteins. Both carry a large net negative charge, but CcP contains 13 more charged residues than Apx and their total net charges (−11 for CcP, −7 for Apx) are different, too. The results of DelPhi calculations (see Table 5) show that while in CcP the dT, in Apx the dA protonation state is stabilized by protein electrostatics. Thus, these studies allow us to draw the same conclusion as the spin calculations. As for the reliability of these calculations it should be mentioned that DelPhi was extremely successful in predicting, for example, pK shifts of protein side chains upon mutation of distant residues,[27] therefore pure electrostatic effects are correctly reproduced. The fact that we used Mulliken charges for the heme group, not reproducing its electrostatic potential outside the van der Waals envelope as well as Kollman ones do, should not alter our conclusions since the heme is identical both in models of CcP and Apx, thus its effect on electrostatics is about the same (see Table 6).

Desolvation energies are practically equal for the corresponding protonation states of the two enzymes, therefore it is the interaction of the charges of the triad with protein charges that causes the difference between the two enzymes. Table 6 summarizes what structural features make Apx especially effective in the solvation of the dA protonation state. We broke down the total electrostatic interaction energy of the dA and dT motif into contributions by all residues within a 500 pm radius of the CG atom of Asp, the Met-172/Ser-160 pair, the heme atoms, and the water/cation binding loop, respectively, for both enzymes. In Apx several of the amino acids and the

Cytochrome C Peroxidase and Ascorbate Peroxidase

J. Phys. Chem. B, Vol. 103, No. 1, 1999 **231**

TABLE 3: Calculated Spin-Density Distribution for the Porphyrin Ring in the dA State of Apx
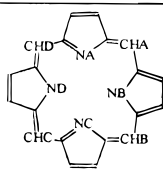
atom name	NA	NB	NC	ND	CHA	CHB	CHC	CHD	total
spin density	0.17	0.14	0.14	0.09	0.14	0.20	0.32	0.10	1.30

TABLE 4: Effect of the Water (WB)- and Cation (CB)-Binding Loops on the Spin-Density Distribution in CcP

	dT	dT + WB	dT + CB
Fe=O	2.05	2.11	1.99
porphyrin	−0.11	−0.06	0.07
proximal Trp	1.05	1.04	1.05

TABLE 5: Solvation Free-Energy Terms (kJ/mol) for the Three Different Protonation States in CcP and Apx As Obtained by Discretized Poisson−Boltzmann Calculations

	CcP			Apx		
	dH	dA	dT	dH	dA	dT
ΔG_{desolv}	86.44	77.41	45.15	83.49	73.31	46.84
ΔG_{int}	−163.73	−155.66	−142.69	−141.57	−184.40	−143.80
ΔG_{tot}	−77.29	−78.25	-97.54	−58.08	−111.09	−96.96

water molecules around Asp (Tyr-190, Gln-204, W-410, W-417, and Lys-209) are ideally positioned to solvate the negative charge of its two oxygen atoms. For example the hydrogen of the OH group of Tyr-190 is 184 pm away from OD1 of Asp-208 forming a strong H-bond with it. Incidentally, this also supports the notion that His is not deprotonated in Apx since the OD1 of Asp, that should abstract a proton from His, is in a favorable and tight H-bond with Tyr-190. The corresponding amino acids of CcP, Phe-202, Met-231, W-332, and Tyr-236 also stabilize the dA state but in an extent less than by a factor of one-third as compared to Apx. The interaction of Met-172 of CcP with the charges of the triad is more effective in the dT state, while Ser-160 of Apx interacts equally well with the dA

and the dT protonation motif but is responsible for keeping in place an extra water molecule (W-417) close to the Asp which contributes to the excess stability of dA.

Heme atoms (including Fe and the active oxygen) stabilize the dA state in both enzymes. Using a model of the engineered CcP, where the potassium-binding loop was present, the electrostatic potential pattern practically did not change as compared to the wild-type enzyme. Electrostatic contribution of the water/cation-binding loop is small in both cases. In CcP the water-containing loop slightly stabilizes the dT protonation state, while in Apx the effect of the cation-binding loop in differentiating between the two protonation states is negligible. This means that the engineered cation-binding loop, similarly as in Apx, does not provide excess electrostatic stabilization for promoting the proton shift in CcP, therefore it should not have a significant effect on the radical location, either.

Figure 3 shows comparison of the electrostatic potential generated by the protein at the atomic sites of the His...Asp...Trp triad of both enzymes in the dA state. It can be seen that the large positive potential at the oxygen atoms of Asp of Apx exceeds those values obtained for CcP, showing that the dA state is indeed favored more strongly by Apx than by CcP.

Discussion

Comparison of experimentally detected radical sites of CcP and Apx (Trp and porphyrin radical, respectively) and the calculated spin-density distributions indicate that the three H-bonded residues of the proximal side are protonated differ-

TABLE 6: Interaction Free Energy (ΔG_{Int} in kJ/mol) of Protein Segments within a Radius of 500 pm from Asp, the Met-172/Ser-160 Pair, the Heme Atoms, and the Water/Cation-Binding Loop with the Charges of the His...Asp...Trp Triad; Corresponding Amino Acids of the Two Enzymes Are Displayed in the Same Row

| CcP				Apx			
side chain	dT	dA	dT−dA	side chain	dT	dA	dT−dA
Side Chains within 500 pm Radius around Asp							
Phe-202	0.43	−1.89	2.32	Tyr-190	0.27	−7.47	7.74
Met-231	0.28	−3.53	3.81	Gln-204	1.29	-8.57	9.86
W-332	−1.49	−9.67	8.18	W-410	−3.34	−12.31	8.9
				W-417	−0.72	−2.01	1.29
Leu-232	−4.75	−1.84	−2.91	Leu-205	−4.98	−5.30	0.32
Tyr-236	−23.42	−21.16	−2.26	Lys-209	−17.28	−19.54	2.26
Thr-234	−14.31	−14.81	0.50	Ser-207	−18.45	−19.24	0.79
subtotal	−43.26	−52.90	9.46	subtotal	−43.21	−74.44	31.23
Met-172	−2.03	0.27	−2.30	Ser-160	−1.67	−1.68	0.01
heme	−7.66	−24.23	16.57	heme	−9.20	−27.93	18.73
water-binding loop				cation-binding loop			
W	0.05	−0.38	0.43	K$^+$	1.80	−2.69	4.49
Ala-176	−12.57	−11.76	−0.81	Thr-164	−26.22	−26.19	−0.03
Gly-192	−19.18	−18.31	−0.87	Thr-180	−21.30	−20.32	−0.98
Thr-199	−0.22	0.77	−0.99	Asn-182	−0.18	0.27	−0.45
Val-197	0.75	0.89	−0.14	Ile-185	0.61	0.93	−0.32
Ala-194	−0.04	0.21	−0.25	Asp-187	−1.90	0.86	−2.76
subtotal	−31.21	−28.58	−2.63	subtotal	−47.19	−47.14	−0.05
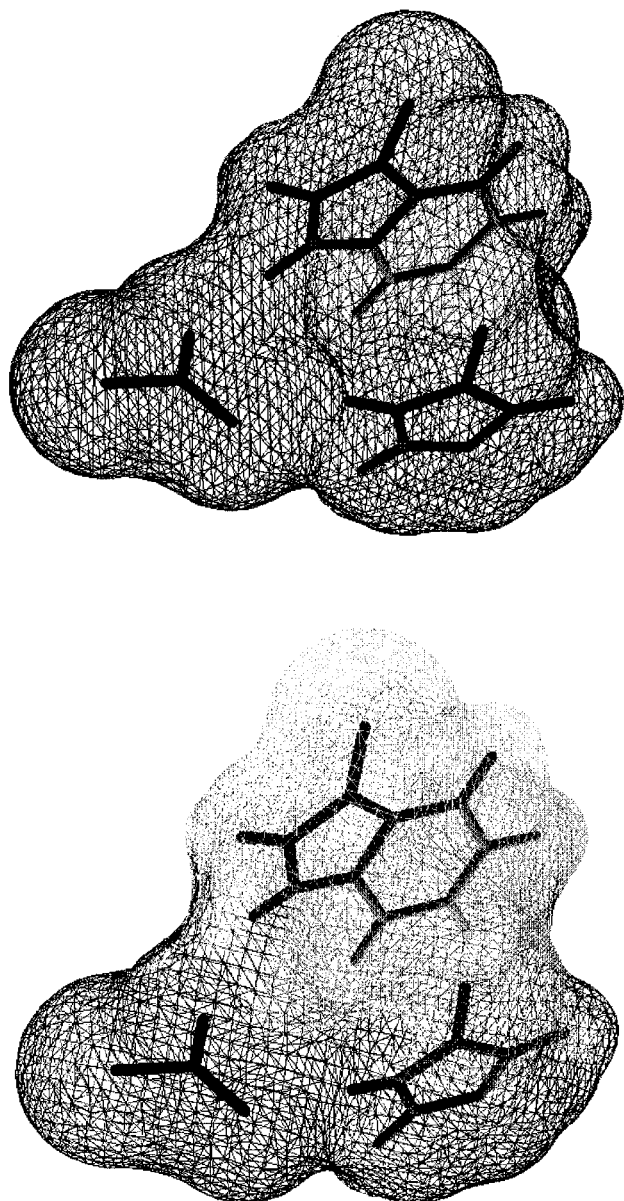
Figure 3. Display of the protein electrostatic potential on the van der Waals envelope of the proximal His...Asp...Trp triad in CcP (left) and Apx (right). The darker regions carry more positive potential.

ently in Compound I of the two enzymes. For CcP the observed Trp radical was reproduced with the dT protonation arrangement; however, the porphyrin radical of Apx was the result of placing the protons according to the dA structure. Despite their similar active sites, the effect of the small differences in the immediate surroundings is reflected in the differing spin-density patterns of the same protonation scheme in the two enzymes.

The resting state of CcP was, by several means,[14,19] shown to contain neutral Asp and Trp side chains and a deprotonated His adjacent to the Fe^{3+} cation (dH protonation scheme). The calculated spin distribution of this state (dH) for CcP coincides with the proposition of Krauss and Garmer that initially a porphyrin radical is formed in Compound I of CcP which later stabilizes in the form of a Trp radical.[14] In the case of Apx the same protonation scheme (dH) had to be excluded from further considerations because of its high energy and very unlikely spin distribution.

On the basis of the present calculations we can state that in CcP eventually His is back-protonated by Asp, Asp itself abstracts the proton from Trp and by this proton transfer the radical is shifted from the initial porphyrin site to the deprotonated Trp. Comparison of this conclusion with experimental results, however, is not straightforward because the experimental results themselves are contradictory concerning the state of the Trp-191 radical of CcP. Krauss and Garmer found that characteristic electronic absorption peaks of Compound I of CcP could only be reproduced by model calculations on neutral benzene and indole radicals.[14] They also state that the proton affinity of the Asp side chain strongly exceeds that of a radical Trp cation. Huyett et al. interpreting ENDOR results concluded in favor of a Trp radical cation, but their evaluation of the results relies on spin-density calculations for the indole cation and neutral radicals.[13] Experimentally observed high spin density on C2 adjoining the nitrogen atom of Trp resembled most the calculated results for a cation radical. However, in our calculations, with the surrounding also included, spin-density values of the neutral Trp radical in CcP also provided the same pattern as the experimentally determined one (Table 2). Goodin and McRee[19] concluded in their EPR study that actually two distributions were sufficient to account for the properties of the Compound I radical of CcP, and proposed that these two states would correspond to the H-bond between Asp-235 and His-175. However, on the basis of our results the two corresponding H-bonded states might be that of dA and dT, along the H-bond between Asp-235 and Trp-191. Moving the proton from Asp-235 to Trp-191 results in all the spin being transferred to the ferryl-oxy center; this state could relax by proton transfer from Trp accompanied by one-third of the total spin being transferred to Trp. Thus the coupling between the ferryl-oxy center and the Trp side chain would be along this latter H-bond. It has also been shown in mutation studies that the D235N mutation introduces significant rearrangement of the free-radical center.[20] This observation could also be easily explained using our model, since an Asn in place of Asp-235 would not be able to deprotonate the adjoining Trp; therefore, the Trp radical could not be formed. Thus, it is reasonable to conclude that the Trp radical is neutral and deprotonated in CcP Compound I according to the dT protonation scheme. In Apx the porphyrin radical of Compound I appears in the dA protonation state, when Trp is again neutral and Asp carries a negative charge.

Including a point-charge mimic of the cation-binding loop of Apx in the model of CcP did not bring drastic changes to the spin-density distribution. DelPhi calculations indicate that the protonation states providing experimentally determined spin distributions are those that are most stabilized by protein electrostatics, as well. The unfavorable desolvation term of dA as compared to dT is not compensated by the interaction energy of dA in CcP; however, the opposite happens in Apx. The negatively charged Asp of dA is extremely well solvated by the protein which makes this state most stable. The different behavior of the two enzymes is caused by the differing nature of the amino acids in the vicinity of the proximal Asp in the two enzymes, especially by the presence of acidic hydrogen atoms of Tyr-190, W-410, and Gln-204 of Apx, appropriately positioned for H-bonding.

Conclusions

Calculations support the proposition that the position of the radical center in Compound I is basically determined by the protonation scheme of the three H-bonded residues on the proximal side of peroxidases. On the basis of our calculations the difference in the behavior of the active state of CcP and Apx can be explained by their different protonation motifs. By comparison to experimental results it was possible to assign a

Cytochrome C Peroxidase and Ascorbate Peroxidase

J. Phys. Chem. B, Vol. 103, No. 1, 1999 **233**

particular protonation state to Compound I of both enzymes. We found that the proximal Trp of CcP is radicalized only if the Trp is deprotonated by the neighboring Asp, while in Apx the Asp^-...$TrpH^0$ pair provides the observed porphyrin radical. Electrostatic calculations demonstrated that the protein environment of the H-bonded triad stabilizes these protonation states, too. It is protein electrostatics that selects the protonation state, the protonation state in turn determines the spin distribution of Compound I.

References and Notes

(1) Saunders: B. C. In *Inorganic Biochemistry*; Eichhorn, G. L., Ed.; Elsevier: Amsterdam, 1973; Vol. 2, p 988.

(2) Tien, M.; Kirk, T. K. *Science* **1983**, *221*, 661.

(3) Pribnow, D.; Mayfield, M. B.; Nipper, V. J.; Brown, J. A.; Gold, M. H. *J. Biol. Chem.* **1989**, *264,* 5036.

(4) Dawson, J. H. *Science* **1988**, *240*, 433.

(5) (a) Mauro, M. J.; Fischel, L. A.; Hazzard, J. T.; Meyer, T. E.; Tollin, G.; Cusanovich, M. A.; Kraut, J. *Biochemistry* **1988**, *27*, 7. (b) Mauro, M. J.; Fischel, L. A.; Hazzard, J. T.; Meyer, T. E.; Tollin, G.; Cusanovich, M. A.; Kraut, J. *Biochemistry* **1988**, *27*, 6243.

(6) Sivaraj, M.; Goodin, D. B.; Smith, M.; Hoffman, B. M. *Science* **1989**, *245*, 738.

(7) Yonetani, T. In *The Enzymes*; Boyer, P. D., Ed.; Academic: New York, 1976; Vol. 13, p 345.

(8) Poulos, T. L.; Fenna, R. E. *Met. Biol.* **1994**, *30,* 25.

(9) Patterson, W. R.; Poulos, T. L. *Biochemistry* **1995**, *34*, 4331.

(10) Patterson, W. R.; Poulos, T. L.; Goodin, D. B. *Biochemistry* **1995**, *34*, 4342.

(11) Bonaqura, C. A.; Sundaramoorthy, M.; Pappa, H. S.; Patterson, W. R.; Poulos, T. L. *Biochemistry* **1996**, *35*, 6107.

(12) Miller, M. A.; Han, G. W.; Kraut, J. *Proc. Natl. Acad. Sci. U.S.A.* **1994**, *91*, 11118.

(13) Huyett, J. E.; Doan, P. E.; Gurbiel, R.; Houseman, A. L. P.; Sivaraja, M.; Goodin, D. B.; Hoffman, B. M. *J. Am. Chem. Soc.* **1995**, *117,* 9033.

(14) Krauss, M.; Garmer, D. R. *J. Phys. Chem.* **1993**, *97,* 831.

(15) Náray-Szabó, G. *J. Biol. Inorg. Chem.* **1997**, *2,* 135.

(16) Abola, E. E.; Bernstein, F. C.; Bryant, S. H.; Koetzle, T. F.; Weng, J. In *Crystallographic Databases − Information Content, Software Systems, Scientific Applications;* Allen, F. H., Bergerhoff, G., Sievers, R., Eds.; 1987; p 107. CcP: Goodin, D. B.; McRee, D. E. *Protein Data Bank Entry* 1CCA.; Apx: Patterson, W. R.; Poulos, T. L. *Protein Data Bank Entry* 1APX.

(17) Walden, S. E.; Wheeler, R. A. *J. Am. Chem. Soc.* **1997**, *119*, 3175.

(18) Ortiz de Montellano, P. R. *Annu. Rev. Pharmacol. Toxicol.* **1992**, *32,* 89.

(19) Goodin, D. B.; McRee, D. E. *Biochemistry* **1993**, *32*, 3313.

(20) Wang, J. M.; Mauro, J. M.; Edwards, S. L.; Oatley, S. J.; Fichel, L. A.; Ashford, V. A.; Xuong, N. H.; Kraut, J. *Biochemistry* **1990**, *29,* 7160.

(21) Edwards, S. L.; Nguyen, H. X.; Hamlin, R. C.; Kraut, J. *Biochemistry*, **1987**, *26*, 1245.

(22) Fülöp, V.; Phizackerley, R. P.; Soltis, S. M.; Clifton, I. J.; Wakatsuki, S.; Erman, J.; Hajdu, J.; Edwards, S. L. *Structure* **1994**, *2,* 201.

(23) Frisch, M. J.; Trucks, G. W.; Schlegel, H. B.; Gill, P. M. W.; Johnson, B. G.; Robb, M. A.; Cheeseman, J. R.; Keith, T.; Petersson, G. A.; Montgomery, J. A.; Raghavachari, K.; Al-Laham, M. A.; Zakrzewski, V. G.; Ortiz, J. V.; Foresman, J. B.; Cioslowski, J.; Stefanov, B. B.; Nanayakkara, A.; Challacombe, M.; Peng, C. Y.; Ayala, P. Y.; Chen, W.; Wong, M. W.; Andres, J. L.; Replogle, E. S.; Gomperts, R.; Martin, R. L.; Fox, D. J.; Binkley, J. S.; Defrees, D. J.; Baker, J.; Stewart, J. J. P.; Head-Gordon, M.; Gonzalez, C.; Pople, J. A. Gaussian94, Revision B.2, Gaussian, Inc.: Pittsburgh, PA, 1995.

(24) Niemz, A.; Rotello, V. M. *J. Am. Chem. Soc.* **1997**, *119*, 6833.

(25) Singh, U. C.; Kollman, P. A. *J. Comput. Chem.* **1984**, *5*, 129.

(26) Sharp, K.; Honig, B. *J. Phys. Chem.* **1990**, *94,* 7684.

(27) Sharp, K.; Honig, B. *Annu. Rev. Biophys. Biophys. Chem.* **1990**, *19,* 301.

(28) DelPhi, Molecular Simulations Inc., 9685 Scranton Rd., San Diego, CA 92121, 1995.